Rotational relaxation characteristics of the monoclinic phase of CCl_4

Mariano Zuriaga,[1,a)] Marcelo Carignano,[2,b)] and Pablo Serra[1,c)]
[1]*Facultad de Matemática, Astronomía y Física, Universidad Nacional de Córdoba, Córdoba, Argentina and IFEG-CONICET, Ciudad Universitaria, X5016LAE Córdoba, Argentina*
[2]*Department of Biomedical Engineering and Chemistry of Life Processes Institute, Northwestern University, 2145 Sheridan Road, Evanston, Illinois 60208, USA*

(Received 21 April 2011; accepted 29 June 2011; published online 25 July 2011)

We present a study of crystalline CCl_4 spanning up to 10 orders of magnitude in time at temperatures ranging from 160 K to 190 K using molecular dynamics simulations. The relaxation process is studied using angular self correlation functions. The results show that each of the four nonequivalent molecules of the monoclinic phase have a particular relaxation time. Two of the molecules relax in an exponential way and the two other molecules have a more complex behavior, especially at the lower temperatures. In all cases, the molecular rotations correspond to quick jumps between equivalent tetrahedral equilibrium positions. Most of these rotations are about the C_3 symmetry axes, however at high temperatures, rotations about the C_2 symmetry axes are observed as well. The waiting time between rotations follows a Poisson distribution. The calculated relaxation times show an Arrhenius behavior with different activation energy for different nonequivalent molecules, in line with recently published findings of nuclear quadrupole resonance experiments. © *2011 American Institute of Physics*. [doi:10.1063/1.3614417]

I. INTRODUCTION

Organic compounds consisting of nearly spherical molecules exhibit an interesting phase behavior between the liquid and the crystal phases. These intermediate phases, in which the molecules can rotate almost freely about their equilibrium lattice positions, are known as plastic phases,[1] and the corresponding compounds are known as plastic crystals or crystals with orientational disorder (OD). OD phases have a characteristic crystalline long range order with respect to the molecular positions but they show disorder in the orientational degrees of freedom.[2]

Halogenomethane compounds $CBr_{4-n}Cl_n$ with $n = 0, \ldots, 4$ are typical examples of OD crystals.[3] These crystals present a series of solid-solid phase transitions before melting that are related to the little hindrance of the reorientational processes. Namely, since the molecules have a roughly spherical shape, they are able to gain rotational degrees of freedom as the temperature is increased.[4] $CBr_{4-n}Cl_n$ compounds crystallize from the melt to a *fcc* plastic phase and transform into an orientationally ordered monoclinic phase on cooling. For CCl_4, the stable phase is monoclinic, although it may crystallize to a metastable *fcc* phase upon cooling form the melt.[5] The low-temperature ordered phases corresponding to all the compounds of this family are isostructural with a crystal having 32 molecules per monoclinic unit cell ($C2/c$). For $CBrCl_3$ and CBr_2Cl_2, the molecular orientations are disordered regarding the position of the Cl and Br atoms.[4,10] These series of compounds are of great interest because they allow a systematic investigation of the effect of molecular symmetry, size, and intermolecular interaction on the phase sequence and reorientational dynamics.[6–9]

For halogenomethanes with T_d molecular symmetry, CCl_4 and CBr_4, a large number of experimental studies[3,11,12,18,28] and some molecular dynamic simulations[6,13–16] have been reported. The dynamics of CBr_4 and CCl_4 in *fcc* phase have been extensively studied, as this phase can be considered to be representative of an orientationally disordered solid. Because the molecules rotate, some macroscopic properties become similar to those found in the liquid phase; therefore, there is interest in understanding to what extent the short-range order of the plastic phase is related of that of the liquid one. A typical rotational relaxation time in both phases is 10^{-12} s.[17–20]

There are very few works that provide direct information about the dynamics of the molecules in the monoclinic phase. One of the first is a ^{13}C NMR study on CBr_4 that showed the change in the dynamics from an essentially diffusive motion in the liquid to a much slower jump motion in the orientationally ordered monoclinic phase with an apparent discontinuity across the *fcc*-monoclinic phase transition.[20] More recently,[21] it has been determined by means of nuclear quadrupole resonance (NQR), that large amplitude molecular reorientational jumps also occur at low temperature for CCl_4, $CBrCl_3$, and CBr_2Cl_2. Moreover, the analysis on the NQR relaxation times in CCl_4 also demonstrated that nonequivalent molecules in the asymmetric unit cell perform reorientational jumps around the molecular axes at different time scales.

In this work, we study the single molecule dynamics of CCl_4 in the monoclinic ordered phase. Using molecular dynamics simulations based on simple intermolecular potentials we obtain, as in the NQR experiments, different relaxation dynamics for the nonequivalent molecules. In order to get close to the relevant experimental regime, the simulations were

a)Electronic mail: zuriaga@famaf.unc.edu.ar.
b)Electronic mail: cari@northwestern.edu.
c)Electronic mail: serra@famaf.unc.edu.ar.

TABLE I. Model parameters and geometry of CCl_4.

	ϵ (kJ/mol)	σ (nm)	q (e)	Geometry (nm)	
C	0.227 6096	0.377 39	−0.696	C–Cl	0.1766
Cl	1.094 5344	0.346 67	0.174	Cl–Cl	0.2884

extended up to 8 μs. The results provide detailed information on the characteristics of the rotational relaxation processes of this monoclinic crystal. In Sec. II, we describe the model and the simulation methodology. In Sec. III, we present the results and their implications; the conclusions are presented in the final section.

II. MODEL AND COMPUTATIONAL DETAILS

In the present work, the CCl_4 molecule is modeled as a rigid nonpolarizable tetrahedron with the carbon atom at its center and a chlorine atom at each of the vertices. This perfect tetrahedral molecule has three equivalent C_2 and four equivalent C_3 symmetry axes. For the C–Cl distance, we used the value 0.1766 nm calculated by Rey *et al.*,[22] and the geometrical constraints fix the Cl-Cl distance to 0.2884 nm. Carbon tetrachloride has been studied in detail using spectroscopic techniques (see Ref. 3 and references therein) and its different crystal structures as a function of temperature are well known. In this work, we focus our attention on the phase II. This is a monoclinic crystal with lattice parameters $a = 2.0181$ nm, $b = 1.1350$ nm, $c = 1.9761$ nm, $\beta = 111.46^\circ$, $Z = 32$, and space group $C2/c$. There are four molecules per asymmetric unit.[3]

Several model potentials for CCl_4 have been proposed.[22] Most of these force fields consist of a combination of Lennard-Jones and Coulombic interactions. The Lennard-Jones parameters are essentially the same for all the models, but very different values for charges have been proposed. We used the charges obtained by *ab initio* calculations and Lennard-Jones parameters presented in reference,[22] which are listed in Table I. Lennard-Jones parameters for the C–Cl interactions were calculated using the combination rules $\epsilon_{ij} = \sqrt{\epsilon_i \epsilon_j}$ and $\sigma_{ij} = (\sigma_i + \sigma_j)/2$.

Molecular dynamics (MD) simulations were performed using the GROMACS v4.0.5 simulation package.[23,24] All simulations were run under NPT conditions, with $N = 512$ molecules (2560 atoms) that correspond to 16 monoclinic unit cells and periodic boundary conditions were applied. The classical Newton's equations were integrated using the leap-frog algorithm with a time step of 0.005 ps. The temperature was maintained constant by coupling the system to a Nose-Hoover thermostat with a time constant of 0.1 ps. The pressure was controlled by the Parrinello-Rahman approach with a time constant of 0.5 ps.

Since this particular system has relaxation times that span over several orders of magnitude, it is necessary to run very long simulations, up to 10 μs. Therefore, it becomes critically important to use the largest possible time step that yields reliable results. In order to determine the optimal settings, we performed a series of test runs varying the time step from 0.001 to 0.1 ps. The results showed that all simulations with time step of 0.005 ps or shorter produced essentially the same output, then this value was adopted for all the production runs. A less critical issue is the treatment of the long range electrostatic interactions. The tetrahedral symmetry of the CCl_4 model molecule implies that its first non-zero electric moment is the octupole. The leading long range electrostatic term decays as r^{-7}; therefore, there is no need to employ time consuming techniques to account for this contribution. This was in fact checked with a short simulation using Ewald summation. The use of the Ewald method produced no appreciable difference in the total electrostatic energy or in the behavior of the system. Therefore, a spherical cut-off at $r = 1$ nm was imposed for all interactions.

III. RESULTS AND DISCUSSION

In order to check the stability of the crystal structure during the simulation, we have calculated a simplified structure factor

$$S_c(\vec{Q}) = \sum_{\alpha,\beta} e^{i\vec{Q}\cdot(\vec{r}_\alpha - \vec{r}_\beta)}, \tag{1}$$

where the sums run only over the carbon atoms of the system. $S_c(\vec{Q})$ was calculated at 186 K for the initial (experimental) and final configurations of the simulations, respectively. In order to avoid some of the complexities derived from the monoclinic unit cell, the structure factor was calculated along certain preferential directions of $\vec{Q}$. Figure 1 shows $S_c(\vec{Q})$ in the range 5–60 nm^{-1}. The diffraction pattern shows Bragg peaks of the simulated crystal that are localized in almost the same positions as the corresponding to the initial crystalline structure. The peaks along the (001), (010), and (100) $\vec{Q}$ directions contain the information to extract $c \sin\beta$, b, and $a \sin\beta$. The experimental values of these lattice parameters are 1.839 nm, 1.135 nm, and 1.878 nm, while the obtained from the last conformation of the simulation at 186 K are 1.848 nm, 1.130 nm, and 1.921 nm, respectively. The discrepancies are smaller than 3%; therefore, the lattice parameters are

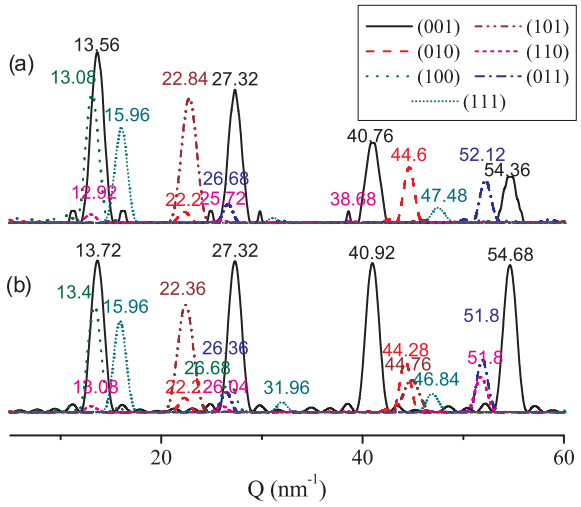

FIG. 1. Structure factor $S_c(\vec{Q})$ against Q for seven directions at (a) $t = 0$ (experimental monoclinic cell) and (b) $t = t_f = 8 \times 10^6$ ps for $T = 186$ K.

preserved throughout the simulations, even at the highest temperature.

As mentioned above, there are four groups of nonequivalent molecules in the unit cell.[3] Each molecule belonging to a given group has the same specific arrangement of neighboring molecules. Therefore, it is reasonable to think that the rotational dynamics is the same for the molecules within a group, but different for molecules belonging to distinct groups. Recent experimental results[21] support this idea. In order to study the differences in rotational dynamics, we classified and divided the molecules of the simulated system in four groups of non-equivalent molecules, each one having $N_I = 128$ molecules.

The single molecule reorientational dynamics has been investigated using angular self-correlation functions, defined as[25]

$$C_l^{I,b}(t) = \frac{1}{N_I}\sum_{i\epsilon I}\left\langle P_l\left(\vec{u}_i^{I,b}(0)\cdot\vec{u}_i^{I,b}(t)\right)\right\rangle. \quad (2)$$

Here, P_l is the l-order Legendre polynomial, $\vec{u}_i^{I,b}$ is a unit vector directed along the C–Cl_b bond (C_3 symmetry axis), $I = 1-4$ denotes each of the four nonequivalent molecules in the asymmetric unit cell, and $b = 1-4$ represents the four C–Cl bonds in the molecule.

In Figure 2, we show the $C_1^{I,b}(t)$ correlation functions for each one of the groups of nonequivalent molecules calculated at three different temperatures. First of all we should note that the angular auto-correlation functions seem not to start at 1 but at a slightly smaller number. This fast decay is shown in the insert of Figure 2 for $T = 185$ K. This initial behavior is originated by the fast molecular librations about the equilibrium positions that relax in times of the order of 1 ps. At the highest temperatures, all $C_1^{I,b}(t)$ decay to zero in times shorter

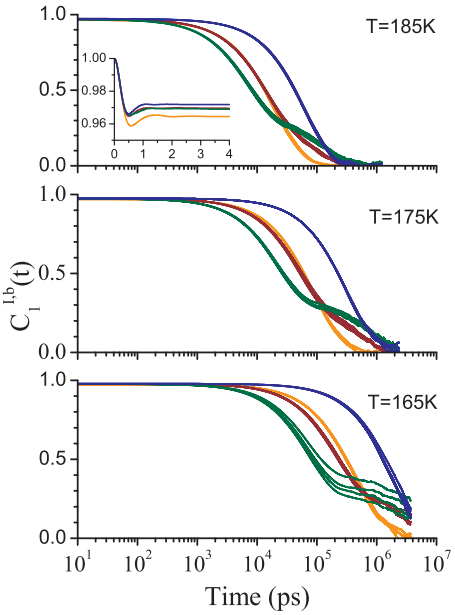

FIG. 2. Sixteen correlation function $C_1^{I,b}(t)$ in orange, brown, green, and blue for the groups $I = 1, \ldots, 4$, respectively. Four lines per group correspond to the four molecular bonds, $b = 1, \ldots, 4$. The inset shows the fast decay of the molecular librations.

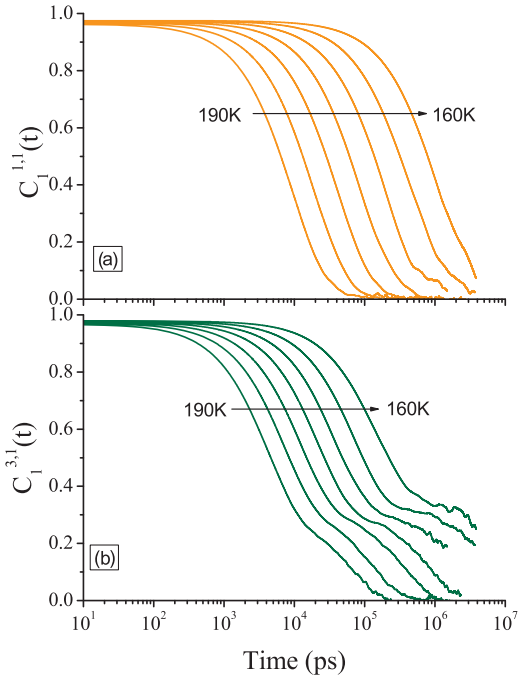

FIG. 3. Correlation function $C_1^{I,1}(t)$ for (a) $I = 1$ and (b) $I = 3$ and temperatures from 160 K to 190 K in steps of 5 K.

than 1 μs, but with different behaviors: exponential for groups $I = 1$ and $I = 4$ (orange and blue) but non-exponential for groups $I = 2$ and $I = 3$ (brown and green). When lowering the temperature, the dynamics slows down for all the groups and the non-exponential behavior is enhanced for groups $I = 2$ and $I = 3$, and is barely insinuated at very long times for group $I = 1$.

The self-correlation functions, $C_1^{I,b}(t)$, are almost independent on the molecular bond (b) for the higher temperatures cases. Indeed, there are four curves in Figure 2 per molecular group, and they practically overlap for 175 and 185 K. At the lowest temperature, this overlap is no longer present, which is more noticeable for group $I = 3$. This different behavior for the same molecule is an indication of an anisotropic rotational preference. In Figure 3, we show the angular self-correlation

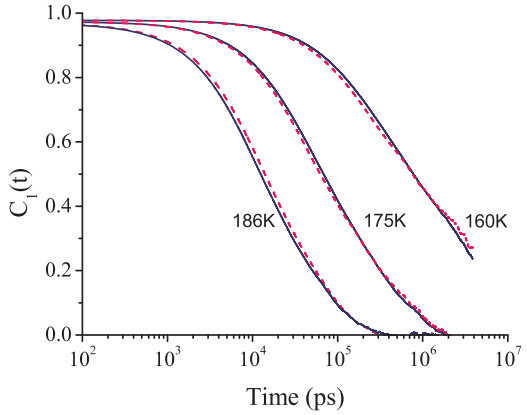

FIG. 4. Correlation functions $C_1(t)$ (continuous lines) for the complete system $N = 512$ molecules and for an arbitrary subset of 128 molecules (dashed lines).

TABLE II. Average number of jumps per molecule × time (jumps/(ps × molecule) calculated from the DMS.

	C_3 jumps				C_2 jumps			
T (K)	g_1	g_2	g_3	g_4	g_1	g_2	g_3	g_4
160	9.29×10^{-7}	1.70×10^{-6}	4.78×10^{-6}	1.99×10^{-7}	0.0	0.0	0.0	0.0
170	5.26×10^{-6}	7.24×10^{-6}	1.72×10^{-5}	1.31×10^{-6}	1.84×10^{-9}	0.0	2.75×10^{-9}	0.0
180	2.43×10^{-5}	2.80×10^{-5}	5.52×10^{-5}	6.79×10^{-6}	4.30×10^{-8}	2.87×10^{-8}	3.44×10^{-8}	4.30×10^{-9}
186	5.91×10^{-5}	6.19×10^{-5}	1.06×10^{-4}	1.83×10^{-5}	2.77×10^{-7}	1.54×10^{-7}	2.77×10^{-7}	3.85×10^{-8}

functions for groups $I = 1$ (orange) and $I = 3$ (green) for a set of temperatures ranging from 160 to 190 K. We plot the results corresponding to only one molecular bond ($b = 1$). For group $I = 1$, the exponential decay persists for a wide temperature range, and some indication of a different behavior could be obseved at very long times for the lower temperatures. For the group $I = 3$, the non-exponential behavior is evident, and it increases systematically with decreasing temperature.

In order to check that the different behaviors of the four correlation functions $C_1^{I,b}(t)$, $I = 1, \ldots, 4$ are effectively associated to four groups of molecules having dissimilar reorientational dynamics, we have performed an additional test summarized in Figure 4. The plot shows a comparison of $C_1(t)$ calculated over the entire system ($N = 512$), and a second autocorrelation function calculated over different aleatory groups of 128 molecules (512/4). The overlap of the two results confirms that the groups of molecules selected according to their crystalline equivalence have indeed different dynamics.

The $C_2(t)$ time correlation functions (not shown) have a similar behavior than the $C_1(t)$ correlation functions. The similarity of the two correlation functions is in agreement with the Ivanov's model for constant amplitude rotational jumps.[26] In this model, the decay constants τ_1 y τ_2 for the correlations functions C_1 and C_2 are given by[27]

$$\tau_1 = \frac{\tau}{1 - \cos\Delta}; \quad \tau_2 = \frac{2\tau}{3(1 - \cos^2\Delta)}, \tag{3}$$

where τ is the average time interval between jumps, and Δ is the constant amplitude jump. Given the symmetry of CCl_4, $\Delta = 109.47^\circ$ is the tetrahedral angle. Then, $\cos\Delta = -1/3$, which implies that $\tau_1 = \tau_2$ as we have obtained from our simulations.

Information about the relaxation processes can be extracted from the trajectories of the four C–Cl bonds for the different groups of molecules. In Figure 5, we display one set of typical trajectories of the four Cl atoms of an arbitrary molecule that belongs to the group $I = 1$. The plotted coordinates are relative to the C atom of the same molecule. The figure shows that the Cl atoms perform quick jumps between equilibrium positions. A detailed analysis of the trajectories shows that the molecular reorientations correspond mostly to 120° jumps about the C_3 symmetry axes. However, for the higher temperatures ($T > 170$ K), some rotations of 180° about the C_2 molecular symmetry axes are also observed (see Table II). A complementary and different representation of this process is displayed in Figure 6. In this case, the trajectory of one of the four C–Cl bonds of a molecule is projected over a sphere. The figure displays a case for each one the four non-equivalent groups at $T = 160$ K and $T = 186$ K. Both representations show that the molecular reorientations consist of sudden jumps of the Cl atoms between equilibrium positions. For the high temperature all groups behave similarly, and the four equilibrium positions are visited. For the lowest temperature, there are two molecular groups that do not visit all the equilibrium positions within the length of the simulation. Indeed, at $T = 160$ K, the mean time between jumps for the molecules of group $I = 4$ is comparable to the total simulation time (see Table II). The particular molecule shown in this case performed just one jump during the simulation; therefore, there are only two spots on the corresponding sphere of Figure 6. On the other hand, the molecules belonging to the group $I = 3$ have a mean time between jumps one order of magnitude shorter than that of group $I = 4$. However,

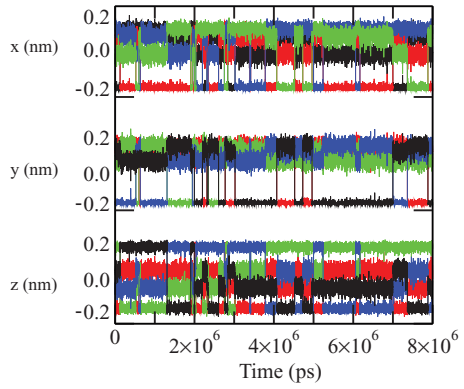

FIG. 5. Coordinates of the Cl atoms as a function of time for an arbitrary molecule of group $I = 1$ and $T = 170$ K. The C atom of the same molecule is used as the reference. Black, red, blue, and green lines correspond to the $b = 1, \ldots, 4$ bonds, respectively.

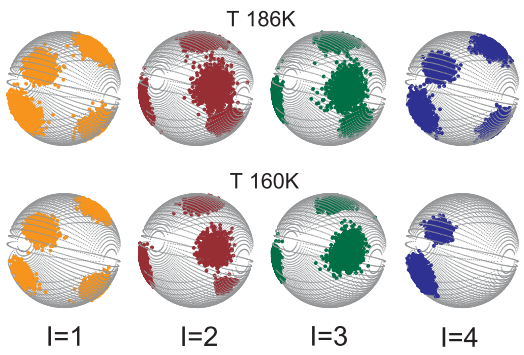

FIG. 6. Spherical proyection of the trajectories of the vectors $\vec{u}^{I,1}$ of one molecule of each group $I = 1, \ldots, 4$ for two temperatures $T = 186$ K and $T = 160$ K.

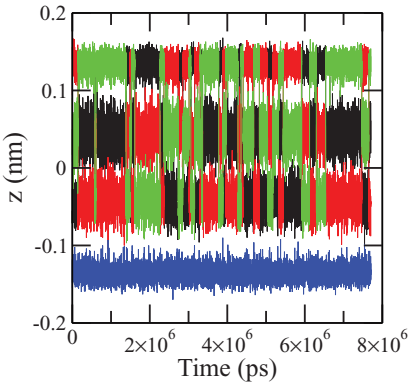

FIG. 7. z coordinates of the Cl atoms as a function of time for an arbitrary molecule of group $I = 3$ and $T = 160$ K. The C atom of the same molecule is used as the reference. Black, red, blue, and green lines correspond to the $b = 1, \ldots, 4$ bonds, respectively.

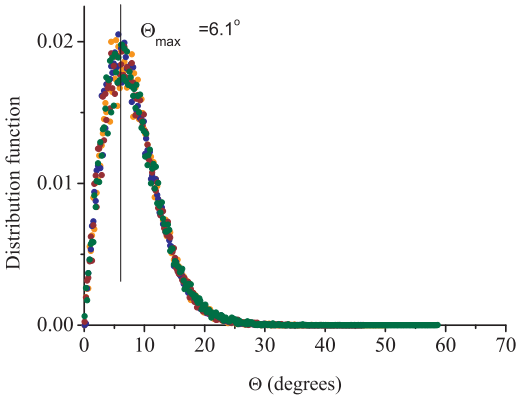

FIG. 8. Distribution of angular desviations, at $T = 175K$, of an arbitrary bond for the four groups $I = 1, \ldots, 4$ in orange, brown, green, and blue, respectively.

as it is shown in Figure 7, one of the Cl atoms of the molecule did not jump, while the other three atoms jumped about fifty times during the entire simulation, in agreement with the values of Table II. That means that, at low temperatures, the reorientations around the different C_3 axes are anisotropic for the group $I = 3$, and the reorientations of 120° around a single C_3 axis remain.

Figure 6 also shows the librations of the molecule about the equilibrium position. The trajectories of the angular deviations of the bond vectors, $\Theta(t)$, contain information that can be related to Raman spectrometry. In Figure 8, we show the distribution for the angular deviations Θ (between jumps) corresponding to $T = 175$ K. The figure, that shows the collapse of the data corresponding to the four non-equivalent groups into the same distribution, has a maximum at $\Theta_{\max} = 6.1^\circ$. Assuming that the librations correspond to a classic oscillator, and recalling the equipartition theorem

$$\langle E_p \rangle = \frac{1}{2} I \omega^2 \langle \Theta^2 \rangle = \frac{1}{2} k_B T , \qquad (4)$$

we can correlate our findings with experimental data. Here, I is the moment of inertia of the molecule and ω is the mean vibrational frequency. Using a value of I calculated from the molecular data[3] and $\omega = 37$ cm^{-1} from Raman spectroscopy,[28] we found at $\langle \Theta^2 \rangle^{1/2} = 5.9^\circ$, in excellent agreement with the predictions of our simulations.

Up to this point, we conclude that the dynamics of the system can be divided in two perfectly identified molecular motions. On one side, there are fast librations characterized by times of the order of 1 ps. On the other side, the molecules experience reorientational jumps; the majority of them about the C_3 symmetry axes. The time scales of the reorientational jumps are in the 0.01–10 μs range.

For regular tetrahedral molecules, Pratt *et al.*[29,30] showed that the correlation functions are exponentials if the reorientational mechanisms (jumps) are symmetric. This is the behavior of groups $I = 1$ and $I = 4$, for which the jump probabilities for all the Cl atoms are the same. Namely, the probability associated to a jump from site i to site j is $\lambda_{i,j} = \lambda$, for all i, j pairs and the correlation time is $\tau = 1/4\,\lambda$. For an asymmetric case, in which one or more $\lambda_{i,j}$ are different from the others, the correlation functions have at least a double and at most a triple exponential decay. This seems to be the behavior of groups $I = 2$ and $I = 3$, as it was described above. In particular, the group $I = 3$ at low temperatures is a limit case of reorientations around just one C_3 axis. In a general asymmetric case, the decay times do not have a simple expression as a function of the jump probabilities $\lambda_{i,j}$. The full asymmetric case is an exception, for which $\tau = 1/3\,\lambda$.[30]

The characteristic time for the molecular reorientational jumps, τ_1, can be calculated from the angular self-correlation functions. The standard definition $\tau_i = \int_0^\infty C_i(t)\,dt$, cannot be easily applied here because of the long correlation times. Only for the higher temperatures, the correlation functions $C_1^{I,b}(t)$ reach zero within the simulated time. A different approach, strictly valid only for exponential decay, consists in assigning τ_1 to the value of time at which $C_1(t)$ decays to $1/e$.[31] This method clearly fails for the cases when the correlation functions are multi-exponentials or develop a plateau. Then we used an alternative method to calculate τ based in the distribution function for the waiting time between molecular jumps. All these three methods are coincident for exponential decay of the correlation functions. The distributions of waiting times between jumps are shown in Figure 9 for $T = 175$ K, for each one of the non-equivalent groups of molecules. The simulation results are consistent with the assumption that the jumps of the molecules are independent Poisson processes. The mean value for the waiting time, τ^I, is easily calculated from the slope of the semi-logarithmic plots. For the cases $I = 1$ and $I = 4$, which correspond to an (almost) exponential decay, the correlation times calculated with the standard definition are in a reasonable agreement with the value obtained from the waiting time distributions. For the other two molecular groups, $I = 2$ and $I = 3$, the mean values of τ^I are in close agreement with time constants that characterize the short time decay of the non-exponential self-correlation functions.

We have determined the reorientational correlation times for the CCl_4 molecules in the temperature range of 160 to 190 K. Existing experimental NQR data cover the range from 100 to 140 K. The reason for the mismatch of the

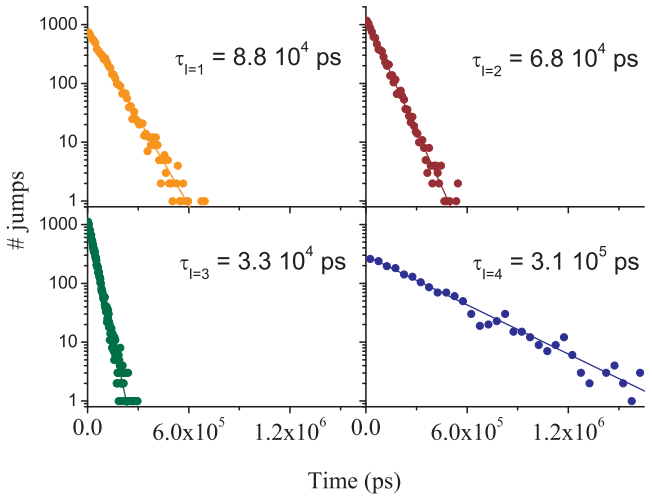

FIG. 9. Distribution functions of the waiting time between molecular jumps at $T = 175$ K for the four groups $I = 1, \ldots, 4$ in orange, brown, green, and blue, respectively.

temperature range is related to the limitations of both techniques. For the simulations, it is excessively expensive to go beyond 10^{-5} s, while the NQR experiments can only probe times longer that 10^{-4} s. In Figure 10, we show the correlation times determined from our MD simulations and those obtained from the NQR experiments.[21] As it was discussed in that reference, the correlation times obtained from the experimental data only allowed to conclude on the existence of at least two groups of molecules with different dynamics. From Figure 10 it can be concluded that there is a reasonable correspondence between the MD and experimental data sets. Experiments and simulations results also show that the system obeys an Arrhenius behavior characteristic of thermally activated processes. The activation energies for the different molecular groups calculated from the simulations are in the range of 30–39 kJ/mol. These values are larger than the experimental activation energies, which are 26 and 29 kJ/mol.

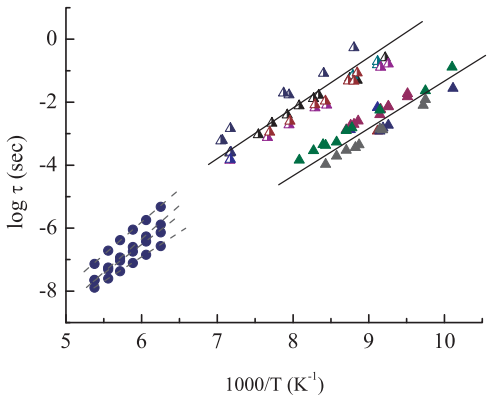

FIG. 10. Average time between molecular jumps from the MD simulations (full blue circles). Experimental values of the correlation times of the molecules reported by Zuriaga *et al.*[21] are aslo shown. Filled and half-filled triangles correspond to molecules with slow and fast dynamics, respectively.

IV. CONCLUSIONS

In the present work, we have investigated the rotational dynamics of CCl_4 in the monoclinic phase by means of MD simulations. Using simple intermolecular potentials we performed simulations spanning over 10 orders of magnitude in time, from fs to μs. Also we observed the molecular librations at the ps time scale. The rotational relaxation processes are observed in the ns time scale for the high temperature limit, and they increase beyond the μs as the temperature decreases.

Using angular self-correlation functions we have identified four different relaxation modes corresponding to the four non-equivalent groups of molecules in the monoclinic phase. The rotational dynamics relaxation processes correspond to tetragonal jumps of the Cl atoms between different equilibrium positions. These jumps are mostly about the C_3 molecular symmetry axes, and for temperatures above 170 K, a few jumps about the C_2 symmetry axes are observed. In all cases, the waiting time between jumps can be well described as a Poisson process, which allows us to calculate the relaxation times even though the full relaxation spans over times longer than our simulations. These results are in line with the NQR findings of Zuriaga *et al.*,[21] indicating the existence of dynamic heterogeneity in the monoclinic phase of CCl_4.

Nonequivalent molecules have different reorientational dynamics that can be distinguished not only by their reorientational correlation times but also for the different behavior of their reorientational time correlation functions. At low temperatures, two of the non-equivalent groups began to develop a plateau in $C_1(t)$. This plateau indicates the slowing down of one type of molecular jumps. This effect could be due to the freezing of the rotation around one of the four molecular axes. The length of these low temperature relaxation times challenges the application of full atomistic simulations, and further understanding on this effect could benefit from the use of different and complementary computational approaches.

ACKNOWLEDGMENTS

M.Z. and P.S. would like to acknowledge SECYT-UNC, CONICET, and MINCyT Córdoba for partial financial support of this project. M.A.C. acknowledges the support of the Network for Computational Nanotechnology (NCN).

[1] N. G. Parsonage and L. A. K. Staveley, *Disorder in Crystals* (Clarendon Press, Oxford, 1978).
[2] J. N. Sherwood, *The Plastically Crystalline State: Orientationaly Disordered Crystals* (Wiley, New York, 1979).
[3] S. Cohen, R. Powers, and R. Rudman, Acta Crystallogr. **B 35**, 1670 (1979).
[4] T. Ohta, O. Yamamuro, and T. Matsuo, J. Phys. Chem. **99**, 2403 (1995).
[5] O. Yamamuro, T. Ohta, and T. Matsuo, J. Korean Phys. Soc. **32**, S839 (1998).
[6] R. Rey, J. Chem. Phys. **126**, 164506 (2007).
[7] P. Negier, J. L. Tamarit, M. Barrio, L. C. Pardo, and D. Mondieig, Chem. Phys. **336** 150 (2007).
[8] M. Barrio, P. Negier, J. L. Tamarit, L. C. Pardo, and D. Mondieig, J. Phys. Chem. B **111**, 8899 (2007).
[9] S. Pothoczki, L. Temleitner, and L. Pusztai, J. Chem. Phys. **132**, 164511 (2010).
[10] O. S. Binbrek, S. E. Lee-Dadswell, B. H. Torrie, and B. M. Powell, Mol. Phys. **96**, 785 (1999).
[11] L. C. Pardo, J. L. Tamarit, N. Veglio, F. J. Bermejo, and G. L. Cuello, Phys. Rev. B **76**, 134203 (2007).

[12]L. Temleitner and L. Pusztai, Phys. Rev. B **81**, 134101 (2010).
[13]I. R. McDonald, D. G. Bounds, and M. L. Klein, Mol. Phys. **45**, 521 (1982).
[14]M. T. Dove, J. Phys. C **19**, 3325 (1986).
[15]I. G. Tironi, P. Fontana, and W. F. Van Gunsteren, Mol. Sim. **18**, 1 (1996).
[16]R. Rey, J. Phys. Chem. B **112**, 344 (2008).
[17]R. Rey, J. Chem. Phys. **129**, 224509 (2008).
[18]K. T. Gillen, J. H. Noggle, and T. K. Leipert, Chem. Phys. Lett. **17**, 505 (1972).
[19]M. More, J. Lefebvre, and B. Hennion, J. Physique **45**, 303 (1984).
[20]B. A. Pettitt and R. E. Wasylishen, Chem. Phys. Lett. **63**, 539 (1979).
[21]M. Zuriaga, L. C. Pardo, P. Lunkenheimer, J. L. Tamarit, N. Veglio, M. Barrio, F. J. Bermejo, and A. Loidl, Phys. Rev. Lett. **103**, 075701 (2009).
[22]R. Rey, L. C. Pardo, E. Llanta, K. Ando, D. O. López, J. L. Tamarit, and M. Barrio, J. Chem. Phys. **112**, 7505 (2000).
[23]D. van der Spoel, E. Lindahl, B. Hess, G. Groenhof, A. E. Mark, and H. J. C. Berendsen, J. Comp. Chem. **26**, 1701 (2005).
[24]B. Hess, C. Kutzner, D. van der Spoel, and E. Lindahl, J. Chem. Theory Comput. **4**, 435 (2008).
[25]S. Kammerer, W. Kob, and R. Schilling, Phys. Rev. E **56**, 5450 (1997).
[26]E. N. Ivanov, Sov. Phys. JETP **18**, 1041 (1964).
[27]K. Seki, B. Bagchi, and M. Tachiya, Phys. Rev. E **77**, 031505 (2008).
[28]A. Anderson, B. H. Torrie, and W. S. Tse, Chem. Phys. Lett. **61**, 119 (1979).
[29]J. C. Pratt, A. Watton, and H. E. Petch, J. Chem. Phys. **73**, 2542 (1980).
[30]J. C. Pratt and A. Watton, J. Phys. C **17**, 5811 (1984).
[31]F. Affouard, E. Cochin, F. Danède, R. Decressain, M. Descamps, and W. Haeussler, J. Chem. Phys. **123**, 084501 (2005).